

Measuring tropospheric water vapor by normalized differential power measurements: an adaptive approach

L. Facheris

Dipartimento di Elettronica e Telecomunicazioni
Università di Firenze
Firenze, Italy
luca.facheris@unifi.it

F. Cuccoli

CNIT Unit at the Dipartimento di Elettronica e
Telecomunicazioni
Firenze, Italy
fabrizio.cuccoli@unifi.it

Abstract— The NDSA (Normalized Differential Spectral Absorption) method is a novel differential measurement way for estimating the total content of water vapor (*IWV*, Integrated Water Vapor) along a tropospheric propagation path between two Low Earth Orbit (LEO) satellites. NDSA is based on the simultaneous measurement of the total attenuation at two relatively close frequencies in the K_u/K bands, and on the estimate of a “spectral sensitivity parameter” that can be directly converted into *IWV*. NDSA is potentially able to emphasize the water vapor contribution, to cancel out all spectrally flat unwanted contributions and to limit the impairments due to tropospheric scintillation. NDSA performance may change with the altitude at which the radio path is located with respect to the Earth. Therefore, after having examined through some simulations accounting for thermal noise at the receiver and tropospheric scintillation effects its measurement performance, we propose here an adaptive approach to the NDSA method in the case of two counter-rotating LEO satellites, based on the estimation of the signal to noise ratio and the change of the central frequency.

I. INTRODUCTION

Remote sensing of tropospheric water vapor is extremely important for both meteorological and climatological applications, since the troposphere contains almost the totality of the atmospheric water vapor. Recently, we introduced the concept and the underlying motivations of NDSA (Normalized Differential Spectral Absorption) measurements for tropospheric water vapor sounding utilizing a couple of LEO satellites, one carrying a transmitter, the other a receiver [1]. As explained in [1], to which the reader is referred for details, the NDSA method is based on the conversion of a spectral parameter that we called “spectral sensitivity”, measured in the K_u/K bands, into the total content of water vapor (hereafter *IWV*, Integrated Water Vapor) along the propagation path between the two LEO satellites. The NDSA method requires the simultaneous measurement of the total attenuation at two

relatively close frequencies ($f_o - \Delta f/2$ and $f_o + \Delta f/2$), symmetrically placed around an ideal reference frequency f_o , and the estimate of the “spectral sensitivity” S , defined as:

$$S = \frac{P_2 - P_1}{\Delta f P_2} \quad (1)$$

where P_1 and P_2 are the received powers corresponding to two simultaneously transmitted tone signals $s_1(t)$ and $s_2(t)$ with frequencies $f_1 = f_o + \Delta f/2$ and $f_2 = f_o - \Delta f/2$, respectively.

The appeal of the NDSA method are its potential to cancel out undesired spectral attenuation contributions that are sufficiently flat over the NDSA measurement bandwidth $[f_o - \Delta f/2, f_o + \Delta f/2]$ and its potential to limit signal impairments that are correlated in time over the same bandwidth, such as those due to tropospheric scintillation [2]. In [1], we showed that spectral sensitivity can be exploited to provide direct estimates of *IWV* along LEO-LEO tropospheric propagation paths in the 15-25 GHz interval. Such analysis was made accounting for the natural variations of the atmospheric conditions at a global scale, assuming ideal measurement conditions (no disturbance at the receiver nor propagation impairments). Simulation were based on a microwave propagation model and on radiosonde data, and they showed the potential of the NDSA approach to provide direct estimates of *IWV* along LEO-LEO satellites links in the troposphere in the 15-25 GHz frequency range, under different atmospheric conditions. NDSA can provide *IWV* estimates directly by means of power measurements, without requiring any external information (for instance, in GPS/MET or LEO-LEO radio occultation the retrieval of water vapor profiles requires at least adequate surface temperature and pressure information and the inversion of the hydrostatic and absorption equations).

In particular, we found that 17, 19 and 21 GHz are the most appealing frequencies for relating S to the *IWV* in the

low troposphere, since they guarantee a high correlation between the two parameters.

Since the number of tropospheric layers crossed by the propagation path decreases with the path altitude (the so called tangent altitude), the NDSA performance changes with the altitude, as a direct consequence of the variation with height of the atmospheric parameters. Indeed, for a given f_o , at the lowest tangent altitudes attenuation is maximum (and quite high) due to the increased water vapor density, and also the differential attenuation increases for the same reason. In general, higher central frequencies are optimal for higher altitudes, while their performance at lower altitudes degrades due to the lower signal to noise ratio caused by attenuation. For a given f_o , the altitude at which such degradation becomes excessive depends on the atmospheric status, which is *a priori* unknown. Therefore, it would be desirable to employ all 3 frequencies simultaneously at all altitudes. However, this would require an excessive amount of power available on board, while even by using a single frequency channel the receive power levels can easily become extremely low due to the distance between the LEO satellites (about 6300 km) and the atmospheric attenuation.

As discussed in this paper, an adaptive approach can be alternatively adopted, where f_o is changed in transmission based on the estimate of the signal-to-noise ratio at the receiver. To demonstrate how such objective can be achieved, we utilized simulations based on standard atmospheric models and accounting for scintillation, defocusing and receiver noise impairments.

II. SIMULATION SETUP

The two transmitted signals can be expressed by:

$$s_i(t) = V_i \exp[j(2\pi f_i t + \phi_i)] \quad i = 1, 2 \quad (2)$$

The tones received on each channel and degraded by propagation effects can be modeled as:

$$r_i(t) = a_i(t) \cdot s_i(t) \cdot \exp\left[j \frac{2\pi}{\lambda_i} l(t)\right] + n_i(t) \quad i = 1, 2 \quad (3)$$

where $a_i(t)$ is an attenuation coefficient; $\exp(j2\pi l(t)/\lambda_i)$ is the Doppler effect due to the relative motion between the two satellites (λ_i being the wavelength of $s_i(t)$ and $l(t)$ the propagation path length); $n_i(t)$ is the additive thermal noise disturbance, assumed as zero-mean, white and Gaussian (AWGN). The noise terms affecting the two channels are assumed as independent with the same power spectral density $\sigma_n^2 = k_B T_{eq}$, where k_B is the Boltzmann's constant, T_{eq} the equivalent noise temperature of the receiver. The noise bandwidth will be referred to as B_{eq} and depends on the cutoff frequency of the receiver lowpass filters (integrators). More specifically, $a_i(t)$ can be written as:

$$a_i(t) = \chi_i(t) L_{F,i}(t) L_{A,i}(t) L_{D,i}(t) \sqrt{G_{T,i} G_{R,i}}, \quad i = 1, 2 \quad (4)$$

where

- $G_{T,i}$ and $G_{R,i}$ are the transmit and receive antenna gains;

- $L_{F,i}(t)$ is the free space propagation loss;

- $L_{A,i}(t)$ is the loss due to absorption by water vapor, oxygen, nitrogen and clouds along the propagation path. It can be computed as the integral of the extinction coefficient along the propagation path (see [1]). In the frequency range considered here, the attenuation factor $L_{A,i}(t)$ significantly varies with frequency at any altitude. $L_{A,i}(t)$ is the only term of interest in (4), since it provides the attenuation information needed for spectral sensitivity measurements.

- $L_{D,i}(t)$ is the defocusing loss, that is due to 'large scale' variations of the atmospheric index of refraction. It can be modeled in general as a power loss depending on the tangent altitude $z(t)$ of the propagation path. The loss is maximum at the lowest altitudes and is assumed independent of frequency. The expression we utilized is obtained experimentally as an average of different atmospheric conditions (z in km) [2]:

$$L_{D,1}(t) = L_{D,2}(t) = 10^{-\frac{1}{2} \exp(-0.089 z(t))} \quad (5)$$

- $\chi_i(t)$ is the tropospheric scintillation disturbance, generated by diffraction effects related to fluctuations of the refraction index [3]. Scintillation introduces random signal fluctuations that can be modeled as a multiplicative noise annoying each of the two tones. It is assumed that $\chi_1(t)$ and $\chi_2(t)$ are wide sense stationary processes with log-amplitude variance σ_χ^2 , defined as:

$$\sigma_\chi^2 = \text{Var} \left[20 \cdot \log_{10} \left(\frac{\chi(t)}{\text{mean}(\chi(t))} \right) \right] \quad (6)$$

The scintillation coefficients χ_1 and χ_2 can be modeled as two correlated log-normal random variables, hence their joint pdf is [4]:

$$p_{\chi_1, \chi_2}(X_1, X_2) = \frac{1}{2\pi\sigma_1\sigma_2\sqrt{1-\rho^2}} \times \exp \left\{ -\frac{1}{2(1-\rho^2)} \left[\left(\frac{\log X_1 - \mu_1}{\sigma_1} \right)^2 - 2\rho \frac{(\log X_1 - \mu_1)(\log X_2 - \mu_2)}{\sigma_1\sigma_2} + \left(\frac{\log X_2 - \mu_2}{\sigma_2} \right)^2 \right] \right\} \quad (7)$$

where μ_1 , μ_2 , σ_1 and σ_2 are the means and standard deviations of the underlying Gaussian variables, whereas ρ is their correlation coefficient. Under the hypothesis that the two channel frequencies are relatively close, it can be assumed that $\mu_1 = \mu_2 = \mu$, $\sigma_1 = \sigma_2 = \sigma$, so that the two marginals $p_{\chi_i}(X_i)$ $i=1,2$ are identical log-normal distributions. The power of χ_i is typically expressed in dB and is related to the variance of the underlying Gaussian as follows:

$$\sigma_{\chi_i}^2 = \text{var}[10 \cdot \log_{10}(\chi_i)^2] = (8.686)^2 \cdot \sigma^2 \quad (8)$$

whereas the average of the scintillation coefficients can be assumed as unitary, i.e. $E[\chi_i] = 1$ (it follows that μ must be chosen as $\mu = -\sigma^2/2$). Since turbulence increases with decreasing altitude, for the sake of simplicity we assumed that σ_χ (in dB) decreases with altitude as follows:

$$\sigma_\chi(z) = \sigma_{\chi 0} \cdot 10^{-0.1084z} \quad (9)$$

where z is in km and $\sigma_{\chi 0}$ is the value of σ_χ at $z=0$.

Spectral sensitivity measurements require the estimation of the powers P_1 and P_2 of the two tones $r_1(t)$ and $r_2(t)$ after having compensated the Doppler phase. As mentioned, the information of interest is contained in $L_{A,i}(t)$. The other terms in (4) either cancel out¹ when the power ratio P_1/P_2 is taken, or must be considered as sources of error for the spectral sensitivity estimates.

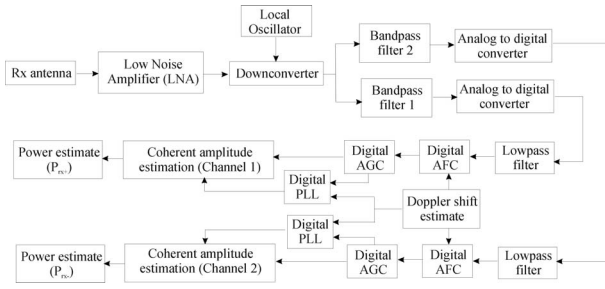


Figure 1. Receiver scheme for spectral sensitivity measurements.

Coherent reception is assumed: Fig. 1 shows the main functional blocks of a receiver that can be utilized for spectral sensitivity measurements. It is composed of two coherent receivers operating at f_1 and f_2 , whose role is to provide the estimates of the powers P_1 and P_2 . After the receiving antenna and the low noise amplifier, the signal is coherently mixed with two tones with frequencies f_1 and f_2 and down-converted to baseband in two separate channels. A PLL (Phase Locked Loop) provides the reference phase for ideal recovery of frequency and phase, including frequency deviation from the nominal value due to Doppler shifts and slow phase variations due to channel phase distortion.

III. SIMULATION RESULTS

Here we analyze the accuracy of spectral sensitivity measurements in the case of a radio link activated between two counter-rotating LEO satellites. We estimated the accuracy of the spectral sensitivity measurements as a function of tangent altitude by means of Monte Carlo simulations (50 runs per case), assuming two reference atmospheric models. These are the Mid Latitude Summer

¹ The difference of the free space losses $L_{F,1}$ and $L_{F,2}$ can be considered negligible for the values of f_0 and Δf considered.

(MLS) and Mid Latitude Winter (MLW). Two atmospheric structures were thus generated, based on the spherical symmetry extension of such vertical profiles. To some extent, such two profiles allow to get an idea of the excursion of atmospheric attenuation in order to evaluate the atmospheric effects on the power levels available at the receiver. A scintillation disturbance process with $\rho=0.98$, following the profile (9) with $\sigma_{\chi 0}=1$ dB was chosen. Since below 12 km tangent altitude the atmospheric attenuation due to water vapor significantly lowers the received power, our analysis starts at that altitude. The link budget and orbit parameters considered are shown in Table 1 (values were selected based on the ESA ACE+ study [5]. Atmospheric attenuation computations were based on the MPM 93 model [6].

TABLE I. LINK BUDGET AND ORBIT PARAMETERS

First LEO satellite orbit altitude	650 km
Second LEO satellite orbit altitude	850 km
Tx Power (on each channel)	33 dBm
Tx Antenna Gain	28 dB
Rx Antenna Gain	28 dB
Implementation Margin	-1 dB
Noise Temp	398 K

Fig. 2 shows the relative measurement accuracy σ_S/S of the spectral sensitivity S for 17, 19 and 21 GHz for the MLS atmospheric profile, versus tangent altitude. In these simulations $\Delta f=400$ Hz was assumed and $B_{eq}=50$ Hz. Fig. 3 plots the corresponding average signal-to-noise ratio at the receiver ($SNR_m=(SNR_1+SNR_2)/2$, where $SNR_i=A_i^2/\sigma_n^2$ is the signal-to-noise ratio over the i -th channel). Observe first of all that the frequency providing the best accuracy changes with altitude: at higher altitudes higher frequencies are preferable. Analogously, observe that the altitude below which spectral sensitivity measurements are excessively degraded (maximum measurement altitude, MMA) depends on the frequency utilized: the higher the frequency, the higher the MMA, that depends on the atmospheric structure.

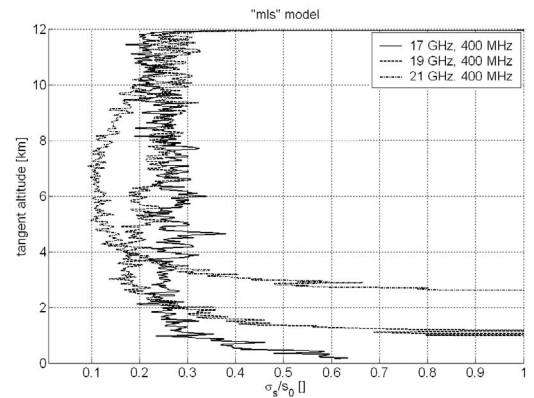


Figure 2. Spectral sensitivity measurement accuracy versus tangent altitude for a Mid Latitude Summer profile

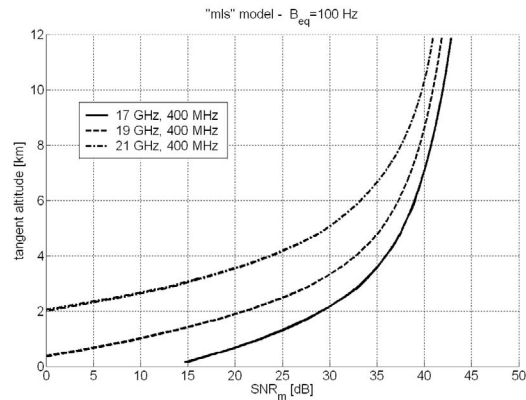


Figure 3. Average signal-to-noise ratio at the receiver for a Mid Latitude Summer profile

However, comparing Fig. 3 with Fig. 2, it can be noticed that MMA is highly related to SNR_m . Indeed, if we assume $\sigma_S/S=0.3$ as the measurement reliability threshold, we note that the corresponding MMA can be found posing $SNR_m=20$ dB as minimum acceptable signal-to-noise ratio threshold. In fact, we would get altitudes of about 3.7, 2.0 and 1.0 km for 21, 19 and 17 GHz, respectively, which are exactly the altitudes where measurement performance falls below acceptability. Fig. 4 and Fig. 5, showing σ_S/S and SNR_m in the same simulation conditions, but for the MLW profile, confirm that the aforementioned 20 dB level of SNR_m can be considered as the threshold that identifies the MMA. In the

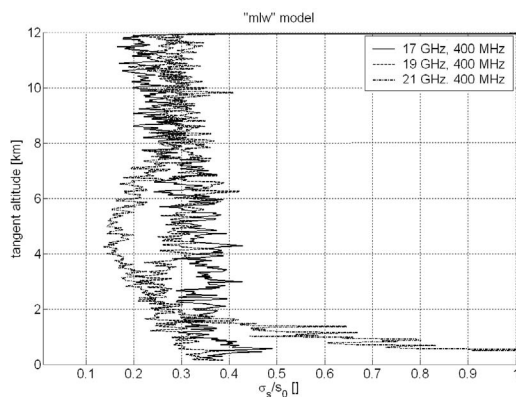


Figure 4. Spectral sensitivity measurement accuracy versus tangent altitude for a Mid Latitude Winter profile

MLW case, indeed, only the 21 GHz channel exhibits SNR_m lower than 20 dB below 2 km altitude, which is the altitude below which the measurement performance degrades. The other two channels (17 and 19 GHz), for which the average signal-to-noise ratio always keeps abundantly over 20 dB, never exhibit performance degradation.

Notice that the 20 dB threshold for SNR_m , while defining the MMA since it represents the minimum level for acceptable values of σ_S/S , is not able to quantify such values.

In fact, these depend mainly on the differential attenuation $\Delta A=10 \log_{10}(P_2/P_1)$ and on the scintillation parameters. Since it is envisaged that the scintillation parameters do not have a significant impact on σ_S/S when $SNR_m \geq 20$ dB is higher than 20, estimating ΔA through power measurements at the receiver would provide reliability indexes of the spectral sensitivity measurements.

Though the error is not estimable through SNR_m , the results shown are definitely exploitable in an adaptive strategy for NDSA measurements based on the estimate of the SNR_m at the receiver to control the frequency switch instants while the radio link between the two counter-rotating LEO satellites is immersing in the atmosphere.

CONCLUSIONS

It is demonstrated by previous works that three central frequencies (namely 17, 19 and 21 GHz) are sufficient to provide the tropospheric water vapor content at any altitude and for any atmospheric condition with sufficient and uniform accuracy. On the other hand, since the atmospheric conditions are unknown, it is unfortunately impossible to define *a priori* the exact range of altitudes at which each of the mentioned frequencies performs better than the other two. Realistically, due to the extreme length of the radio path between the two LEO satellites and to the additional attenuation caused by the crossing of the atmosphere, it is arduous if not impossible to share the available power among three separate transmitters. A much more efficient strategy would be to switch the available power among three transmitters working at the mentioned frequencies, after having detected the MMA through the SNR_m estimate at the receiver, provided that a feedback channel is available to communicate with the transmitting LEO satellite.

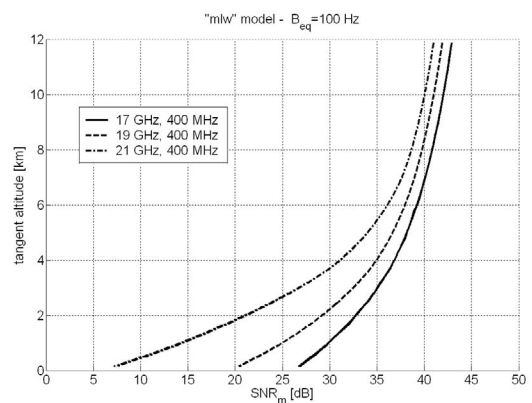


Figure 5. Average signal-to-noise ratio at the receiver for a Mid Latitude Winter profile

The role of ΔA in the estimation of the measurement accuracy of S deserves further investigations. In fact, a theoretical expression (not reported in this paper for simplicity) can be derived for σ_S/S , depending on the received powers, on the noise power and on the scintillation parameters. Such expression shows that when SNR_m takes

realistic values (below 30 dB), σ_y/S is scarcely dependent on the scintillation parameters.

REFERENCES

- [1] F. Cuccoli, L. Facheris, "Normalized Differential Spectral Attenuation (NDSA): a novel approach to estimate atmospheric water vapor along a LEO-LEO satellite link in the Ku/K bands", IEEE Transactions on Geoscience and Remote Sensing, Vol. 44, pp. 1493-1503, 2006
- [2] M. Bonnedal, M. Emardson and J. Wettergren, "Explorer Core Mission – WATS, Instrument description, Final Report", Saab Ericsson Space AB, Document No: P-WATS-REP-0002-SE, Gothenberg, Sweden, 2001
- [3] F. Cuccoli, L. Facheris, A. Freni, E. Martini, "The impact of tropospheric scintillation in the Ku/K bands on the communications between two LEO satellites in a radio occultation geometry"; IEEE Transactions on Geoscience and Remote Sensing, Vol. 44, pp. 2063-2071, 2006
- [4] N.L. Johnson, S. Kotz, "Distributions in Statistics: Continuous Multivariate Distribution" Wiley, New York., 1972
- [5] A. S. Nielsen et al., "Characterization of ACE+ LEO-LEO Radio Occultation Measurements", Final report ESTEC contract No. 16743/02/NL/FF, March 2005
- [6] Liebe H.J., G.A. Hufford, M.G. Cotton "Propagation Modeling of Moist Air And Suspended Water/Ice Particles at Frequencies below 1000 GHz", in AGARD 52nd Specialists Meeting of the Electromagnetic Wave Propagation Panel on "Atmospheric Propagation Effects through Natural and Man-Made Obscurants for Visible to MM-Wave Radiation", Palma de Mallorca, Spain, May 1993